Hindawi Publishing Corporation
Journal of Nanomaterials
Volume 2012, Article ID 592147, 8 pages
doi:10.1155/2012/592147

Research Article

Preparation and Hydrogen Storage Properties of Mg-Rich Mg-Ni Ultrafine Particles

Jianxin Zou,[1,2] Haiquan Sun,[1] Xiaoqin Zeng,[1,2] Gang Ji,[3] and Wenjiang Ding[1,2]

[1] *Shanghai Engineering Research Center of Magnesium Materials and Applications and National Engineering Research Center of Light Alloy Net Forming, Shanghai Jiao Tong University, Shanghai 200240, China*
[2] *State Key Laboratory of Metal Matrix Composites, School of Materials Science and Engineering, Shanghai Jiao Tong University, Shanghai 200240, China*
[3] *Unité Matériaux Et Transformations (UMET), CNRS UMR 8207, Université Lille 1, 59655 Villeneuve d'Ascq, France*

Correspondence should be addressed to Jianxin Zou, zoujx@sjtu.edu.cn

Received 29 August 2012; Accepted 16 October 2012

Academic Editor: Kemin Zhang

In the present work, Mg-rich Mg-Ni ultrafine powders were prepared through an arc plasma method. The phase components, microstructure, and hydrogen storage properties of the powders were carefully investigated. It is found that Mg_2Ni and $MgNi_2$ could be obtained directly from the vapor state reactions between Mg and Ni, depending on the local vapor content in the reaction chamber. A nanostructured $MgH_2 + Mg_2NiH_4$ hydrogen storage composite could be generated after hydrogenation of the Mg-Ni ultrafine powders. After dehydrogenation, MgH_2 and Mg_2NiH_4 decomposed into nanograined Mg and Mg_2Ni, respectively. Thermogravimetry/differential scanning calorimetry (TG/DSC) analyses showed that Mg_2NiH_4 phase may play a catalytic role in the dehydriding process of the hydrogenated Mg ultrafine particles.

1. Introduction

Mg-based alloys and composites are believed to be promising candidates as hydrogen storage carriers due to their high hydrogen storage capacity (7.6 wt% for MgH_2 and 3.6 wt% for Mg_2NiH_4), great abundance, and low cost [1]. However, the sluggish hydrogen sorption kinetics and high operating temperature of Mg (>573 K) limit its practical applications. Different methods, such as alloying, catalyst addition, and nanocrystallization, have been used to improve the hydrogen thermodynamics and sorption kinetics of Mg [2–4]. Consequently, various Mg-based alloys, composites, and compounds have been developed with superior hydrogen sorption kinetics over pure Mg. Among those Mg-based materials, Mg_2Ni intermetallic compound is well known to form Mg_2NiH_4 hydride with high reaction rate, which has a hydrogen storage capacity of 3.6 wt% [1]. However, it is difficult to obtain Mg alloys with accurately desirable compositions by conventional melt-cast methods due to following reasons: (1) Mg has low melting point (923 K) and high vapor pressure (133 Pa at 878 K); (2) Mg is quite active in the presence of oxygen. Especially in the case of Mg-Ni binary system, casting is quite difficult because of the large difference in melting point between Ni (1728 K) and Mg (923 K). Furthermore, based on the binary phase diagram [5, 6], single phase Mg_2Ni cannot be simply obtained by casting as a phase separation occurs during solidification.

Mechanical alloying (MA) method has been widely used to produce nanostructured alloys or composites, especially to produce amorphous and nanocrystalline Mg_2Ni alloys. However, it usually takes a long time to prepare alloys by the MA method, the sample can be contaminated during the milling process, oxidation occurs even in a protective atmosphere [7]. Moreover, it is difficult to obtain a homogenous sample by the MA method [8]. It is known that nano- or ultrafine particles have a lowered melting point because of the small size and large specific surface area of the particles, which implies a possibility of preparing the Mg_2Ni compound by using magnesium and nickel nanoparticles. Lio et al. synthesized Mg_2Ni intermetallic nanoparticles by a two-step method [9]. First, Mg and Ni nanoparticles were prepared by hydrogen plasma-metal reaction. Second,

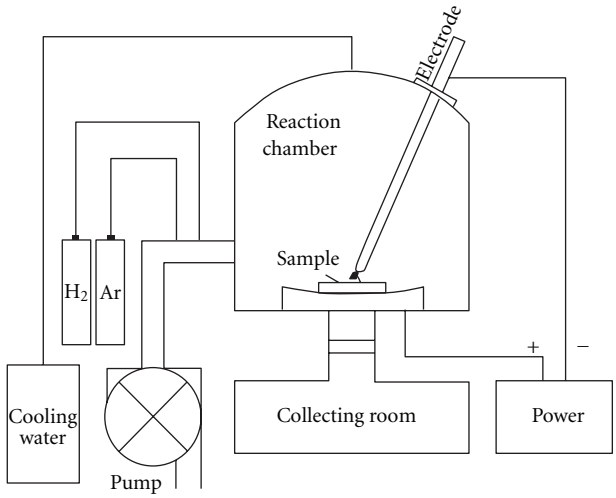

Figure 1: Schematic illustration of the DC arc plasma evaporation equipment.

the mixture of Mg and Ni nanoparticles in a 2 : 1 molar ratio was compressed into a pellet and was heated up to 623 K under a hydrogen pressure of about 40 bar to react with hydrogen. It is established that at 553 K and 3 MPa hydrogen pressure, Mg_2NiH_4 can be generated, and Mg_2Ni intermetallic phase was obtained with high productivity after hydrogen desorption. The obtained Mg_2Ni compound has excellent hydrogen storage properties and can absorb hydrogen to its maximum capacity in the first cycle at a high speed without any activation. Its excellent performance is due to the ultrafine particle size, large surface area, and internal defects.

In this paper, we have attempted the direct preparation of Mg-Ni composite ultrafine particles through vapor state reactions by using a DC arc plasma method. This process is similar to the in-flight plasma processes, which injected the metal powders into the plasma flame leaving the gasification. In this process, the metal vapor cooled down rapidly after leaving the plasma flame, reached saturation, then condensed and formed nano- or ultrafine powders [10].

2. Experimental

2.1. Sample Preparation. The Mg-Ni ultrafine powders were prepared using an arc plasma evaporation apparatus. Figure 1 shows a schematic illustration of the experimental equipment. It mainly consists of a reaction chamber and a collection room. Mg-Ni ultrafine particles were prepared by arc evaporation of the mixture of magnesium and nickel powders. Commercially available Mg and Ni powders with 99.9 wt% in purity and 100 μm in particle size were delicately mixed in a molar ratio of 1 : 2. The mixed powders were then compressed at room temperature to form cylinders with 10 mm in diameter and 7 mm in height by an uniaxial compressor under a pressure of 25 MPa. These cylinders, as anode materials, were put into the reaction chamber filled with mixed 0.75 atm Ar + 0.05 atm H_2 gas after the chamber was evacuated to 5×10^{-2} Pa. The DC current is set at 140 A during arc evaporation. Before the Mg-Ni ultrafine particles were taken out from the reaction chamber, they were slowly passivated with a mixture of argon and air to prevent the particles from burning in air.

2.2. Characterization. The phase identification of the Mg-Ni nanoparticles before and after hydrogen absorption was carried out by X-ray diffraction (XRD) using a D/max 2550VL/PCX apparatus equipped with Cu-Kα radiation source. The morphology and microstructure of the powders were observed by using a JEM-2100 transmission electron microscope (TEM), operated at 200 kV. The composition of the Mg-Ni powders was analyzed by inductive coupled plasma emission spectrometer (ICP). A conventional Sieviet-type pressure-composition-temperature (P-C-T) apparatus, which means measuring hydrogen content versus pressure by recording the change of gas pressure in a constant volume, was used to test the hydrogen sorption properties of the Mg-Ni ultrafine powders. The testing temperatures were set at 400°C, 375°C, 350°C and 325°C. The hydrogen desorption property of the prepared powders was analyzed by thermogravimetry/differential scanning calorimetry spectroscopy (TG/DSC) technique.

3. Results and Discussions

3.1. XRD Analysis. Figures 2(a), 2(b), and 2(c) show the XRD patterns of the as- prepared Mg-Ni ultrafine particles, the samples obtained after the hydrogen absorption and after desorption, respectively. From Figure 2(a), it is seen that the main phases of the Mg-Ni ultrafine particles prepared by DC arc plasma are Mg and Ni, with a small amount of MgO. Besides, the presence of Mg_2Ni and $MgNi_2$ phases is also detected. The peaks corresponding to $MgNi_2$ phase are fairly weak, indicating that the volume content of Mg_2Ni in the powders is very low. The MgO phase was formed when the Mg-Ni nanoparticles were passivated in the mixture of argon and air. The MgO layer at the surface of the magnesium particles can effectively prevent the further oxidation or even burning of the Mg particles when exposed to air. The existence of Mg_2Ni and $MgNi_2$ shows that the following reactions have occurred during the arc plasma evaporation:

$$2Mg + Ni \longrightarrow Mg_2Ni \quad (1)$$

$$Mg + 2Ni \longrightarrow MgNi_2 \quad (2)$$

These reactions occurred in vapor state depending on the local vapor concentrations of Mg and Ni. Indeed, Mg has much higher vapor pressure than Ni at the same temperature, resulting in the generation of a vapor rich in Mg during arc evaporation. ICP analysis shows that the average Mg and Ni content in the Mg-Ni ultrafine powders is 7 : 1 in molar ratio, much higher than the ratio 1 : 2 in the original mixture. However, the local vapor content may not be homogeneous during arc evaporation of the Mg-Ni mixture. Ni concentration might be higher than Mg in local regions inside the plasma. As a result, both reaction (1)

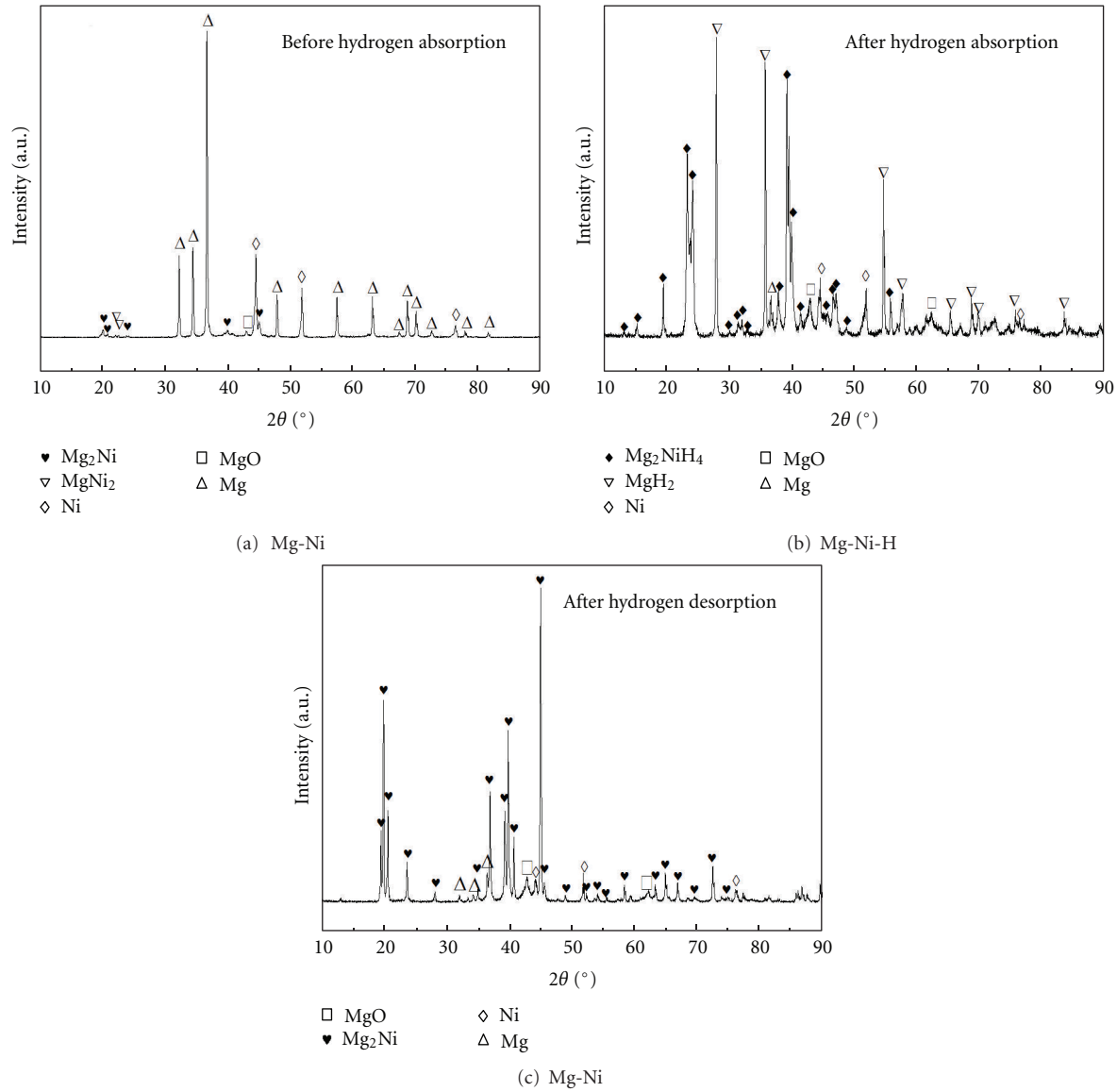

Figure 2: X-ray diffraction patterns of Mg-Ni ultrafine-particles (a), Mg-Ni ultrafine particles after hydrogen absorption at 400°C, 4 MPa, (b), and Mg-Ni ultrafine particles after hydrogen desorption (c).

and reaction (2) could occur in the mixed vapor, leading to the formation of Mg_2Ni and $MgNi_2$ phases. As the vapor is highly rich in Mg, reaction (1) should be more important than reaction (2). As a result, the amount of Mg_2Ni should be higher than the amount of $MgNi_2$. The fact that the majority phases in the Mg-Ni ultrafine powders are pure Mg and Ni indicates that most of Mg and Ni vapors do not react with each other during evaporation. It has been established that the evaporation rate of metals plays a major role for the generation of the metal particles. According to the Ohno's model, the vapor generation rate of a metal through hydrogen plasma reaction method is proximately proportional to its reaction parameter, R_p, which can be expressed by the following equation:

$$R_p = \left(-\frac{\Delta H_r}{L_s}\right)\left[\frac{N_{H2}(T)}{N_{H2}(273)}\right], \quad (3)$$

where H_r is the reaction enthalpy between metal and hydrogen, L_s is the heat of vaporization of the metal at the temperature T, and N_{H2} (T) and N_{H2} (273) are densities of the hydrogen molecules in the metal at temperature T and 273 K. By inputting parameters for Mg and Ni into (3), it is estimated that $R_p = 1$ for Mg and $R_p = 0.17$ for Ni. The large difference in R_p values indicates that the evaporation rate for Ni is much lower than that for Mg. This is consistent with the ICP result for which the Ni content in the composite is lower than that in the mixed powders before arc evaporation.

From the XRD pattern in Figure 2(b), it can be seen that most of the Mg-Ni powders have transformed into MgH_2 and Mg_2NiH_4 hydrides after the hydrogen absorption at 400°C and 4 MPa. The mechanism for the formation of Mg_2NiH_4 hydride is thought to be the reaction (4)

followed by reaction (5) occurred during the isothermal period:

$$Mg + H_2 \longrightarrow MgH_2 \quad (4)$$

$$2MgH_2 + Ni \longrightarrow Mg_2NiH_4 \quad (5)$$

As the atomic ratio of Mg : Ni is 7 : 1 in the Mg-Ni ultrafine powders, the reactions (4) and (5) can be combined together into reaction (6). That is, when Mg-Ni ultrafine powders are completely hydrogenated, the molar ratio of MgH_2 to Mg_2NiH_4 should be around 5 : 1:

$$Mg_7Ni + 7H_2 \longrightarrow 5MgH_2 + Mg_2NiH_4 \quad (6)$$

There is still a small amount of Mg phase observed in the sample after hydrogenation at 400°C, as seen in Figure 2(b). This is due to the fact that some relatively large Mg particles cannot be completely hydrogenated. It is observed from Figure 2(c) that after hydrogen desorption, MgH_2 decomposes completely and transforms into Mg, and Mg_2NiH_4 transforms into Mg_2Ni compound, as described by the following reaction:

$$Mg_2NiH_4 \longrightarrow Mg_2Ni + 2H_2 \quad (7)$$

This principle of the reactions (4), (5), and (7) is used to prepare Mg_2Ni compound by Shao et al. [12, 13]. Comparing Figures 2(a) and 2(b), it is worth noting that the diffraction peaks of $MgNi_2$ disappeared after hydrogen absorption. It is believed that $MgNi_2$ should react with MgH_2 to form Mg_2NiH_4 in the presence of high temperature and hydrogen atmosphere, as described by the following reaction:

$$3MgH_2 + MgNi_2 + H_2 \longrightarrow 2Mg_2NiH_4 \quad (8)$$

3.2. TEM Observations of the Mg-Ni Ultrafine Particles. Figures 3(a), 3(b), and 3(c) show typical bright field TEM micrographs of Mg-Ni composite powders before hydrogen absorption, the samples obtained after hydrogen absorption and after hydrogen desorption, respectively, with corresponding selected area electron diffraction (SAED) patterns. From Figure 3(a), it is observed that most of the particles have quasispherical shape with the particle size ranges from 50 to 600 nm. The corresponding SAED pattern consists of rings and overlapped dispersed spots. The rings are identified to be Mg and MgO phases. However, the spots are not indexed and could correspond to the Ni, Mg_2Ni, and $MgNi_2$ phases based on the result of XRD analysis (Figure 2(a)). Normally, Mg can be directly evaporated into gaseous atoms before melting in the high temperature plasma. This is due to the low melting point and small latent heat of evaporation for Mg. The fast vapor generation rate of the Mg results in the formation of relatively large particles [14]. After hydrogenation at 400°C in 4 MPa hydrogen atmosphere, MgH_2 and Mg_2NiH_4 phases formed in the composite. The typical morphology of these hydrides is shown in Figure 3(b). The particles became transparent having size in the range between 50 and 200 nm, smaller than the Mg particles shown in Figure 3(a). In the corresponding SAED pattern, diffracted rings belonging to MgH_2, Mg_2NiH_4, MgO, and Mg phases can be detected. It is found from Figure 3(c) that after 4 hydrogen absorption and desorption cycles, those large Mg particles have been cracked and broken into smaller particles. The corresponding SAED pattern is mainly composed of well-defined rings belonging to pure Mg. Besides this, MgO and Mg_2Ni are also identified. Compared with that of the as-prepared particles obtained using the same SAED aperture (Figure 3(a)), it indicates the grain refinement of Mg particles after hydrogen sorption cycles. The grain refinement of Mg particles is expected to benefit from the hydrogen storage properties owing to the increased surface areas and reduced diffusion length for hydrogen. As a consequence of the reduction in particle size, fresh surface was generated during the hydriding/dehydriding cycles. The presence of new surfaces makes the Mg particles easier to be oxidized. As a result, the amount of MgO increases after hydrogen sorption cycles, as can be observed from the comparison between diffraction peaks of MgO phase in Figures 2(c) and 2(a).

3.3. Hydrogen Storage Properties. Figure 4 shows the P-C-T curves of the hydrogen absorption-desorption processes for the Mg-Ni ultrafine particles at 400°C, 375°C, 350°C, and 325°C. The data obtained from the P-C-T measurements are summarized in Table 1. Two plateaus of absorption and desorption are clearly visible on each profile. According to the XRD results given above, two types of hydrides, MgH_2 and Mg_2NiH_4, formed after hydrogenation. Therefore, the two plateaus of the absorption and desorption are attributed to the formation and decomposition of MgH_2 and Mg_2NiH_4. According to previous investigations on the Mg-rich Mg-Ni composite materials, the low plateaus are due to hydriding and dehydriding of Mg, while the high plateaus are the results of hydriding and dehydriding of Mg_2Ni [15, 16]. The maximum hydrogen absorption capacities at 400, 375, 350, and 325°C are 3.16, 3.05, 2.97, and 2.96 wt%, respectively, which are even lower than the theoretical value of 3.6 wt% for Mg_2Ni. This is due to the existence of MgO, the residual Mg and Ni in the hydrided Mg-Ni composite, as shown in Figure 2(b). Indeed, some large magnesium particles cannot be completely hydrogenated. From these PCT data, the van't Hoff plots ($\ln P$ versus $1000/T$) for the Mg-Ni composite are drawn in Figure 5. According to the linear fitting lines from the experimental data, the van't Hoff equations for the hydrogenation are $\ln(P_{low}) = -10/T + 15.16$ for Mg and $\ln(P_{high}) = -7.77/T + 12.27$ for Mg_2Ni. The van't Hoff equations for the dehydrogenation are $\ln(P_{low}) = -9.31/T + 13.84$ for Mg and $\ln(P_{high}) = -7.96/T + 12.23$ for Mg_2Ni. Therefore, the obtained values of the hydride formation enthalpies (ΔH_{ab}) are −83.1 kJ/mol for Mg and −64.6 kJ/mol for Mg_2Ni, while the dehydrogenation enthalpies (ΔH_{de}) are 77.4 kJ/mol for Mg and 66.2 kJ/mol for Mg_2Ni. These hydrogenation and dehydrogenation enthalpies of Mg and Mg_2Ni phases agree well with the values reported in the literature, for example, about −66.3 kJ/mol H_2 for hydrogenation of Mg_2Ni [10, 17] and −74.5 kJ/mol H_2 for hydrogenation of Mg [18].

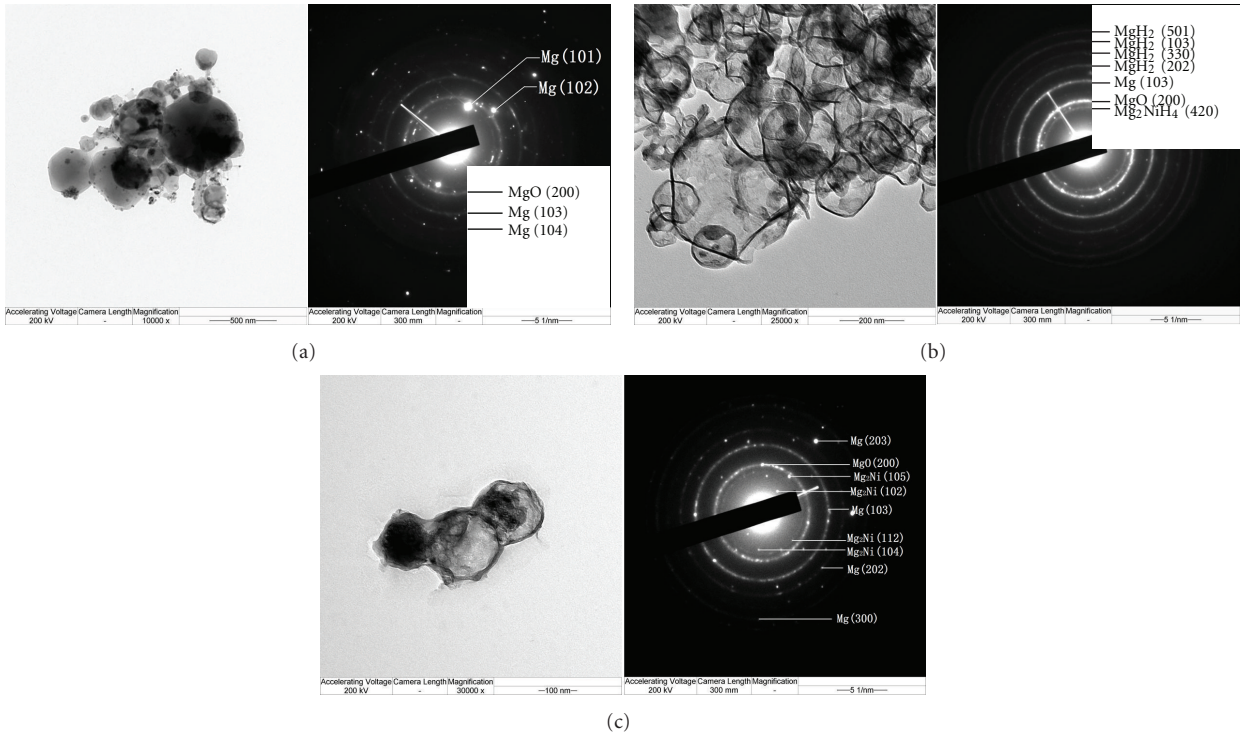

FIGURE 3: Bright field TEM micrographs of Mg-Ni nanoparticles before hydrogen absorption with SAED patterns inset (a), after hydrogen absorption with SAED patterns inset (b), and after hydrogen desorption with SAED patterns inset (c).

TABLE 1: The data of P-C-T tests.

Temperature/°C	Maximum H_2 absorption/wt%	Low plateau of absorption/MPa	Low plateau of desorption/MPa	High plateau of absorption/MPa	High plateau of desorption/MPa
325	2.96	0.195	0.173	0.464	0.338
350	2.97	0.433	0.329	0.840	0.570
375	3.05	0.792	0.645	1.347	0.995
400	3.16	1.259	0.946	1.974	1.457

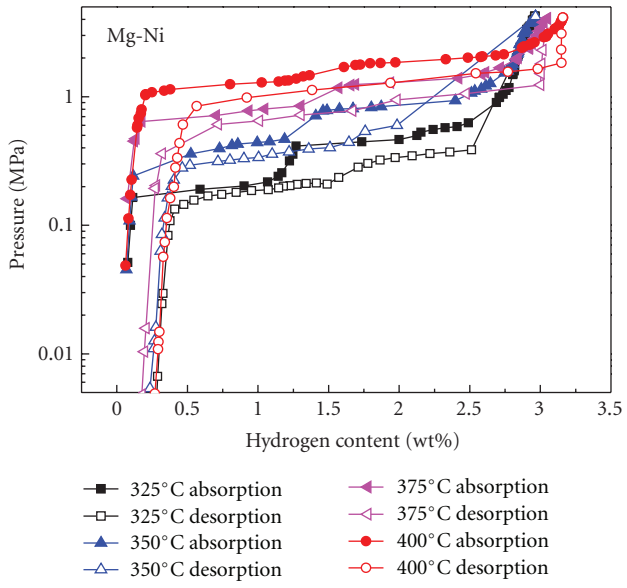

FIGURE 4: P-C-T curves of Mg-Ni ultrafine particles measured at 400°C, 375°C, 350°C and 325°C.

Figure 6 shows the TG/DSC curves of the hydrided Mg-Ni composite obtained in 4 MPa hydrogen atmosphere at 400°C. It is observed that three endothermic peaks appeared on the DSC curve measured from room temperature to 500°C. The small peak in the temperature range between 235°C and 250°C comes from the phase transformation of Mg_2NiH_4 from its low temperature form to its high temperature form [19]. While in the same temperature range, TG curve does not show any mass loss. Two strong endothermic peaks in the high temperature range between 365°C and 425°C are observed on the DSC curve together with a mass loss of 3.3 wt%. They result from the dehydriding of Mg_2NiH_4 and MgH_2. In order to understand the dehydriding processes of the hydrogenated Mg-Ni composite, a partially hydrogenated sample is prepared and studied by using DSC technique. The sample is hydrogenated at 350°C with 0.89 wt% of hydrogen absorption. Figure 7 shows the XRD pattern of the partially hydrogenated composite. From Figure 7, one can see that both MgH_2 and Mg_2NiH_4 phases exist after absorbing 0.89 wt% of hydrogen. The intensity of peaks from MgH_2 is relative higher than that of the Mg_2NiH_4 phase, indicating that the main product in this partially

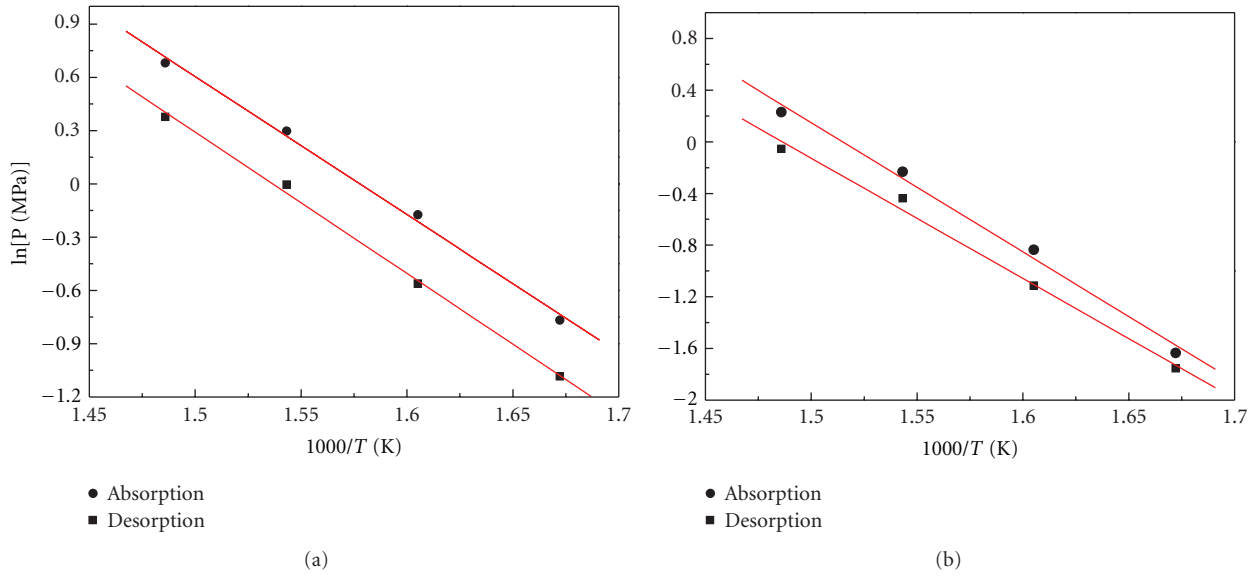

Figure 5: Van't Hoff plots based on the low plateaus (a) and high plateaus (b) on PCT curves for hydrogenation and dehydrogenation of the Mg-Ni composite.

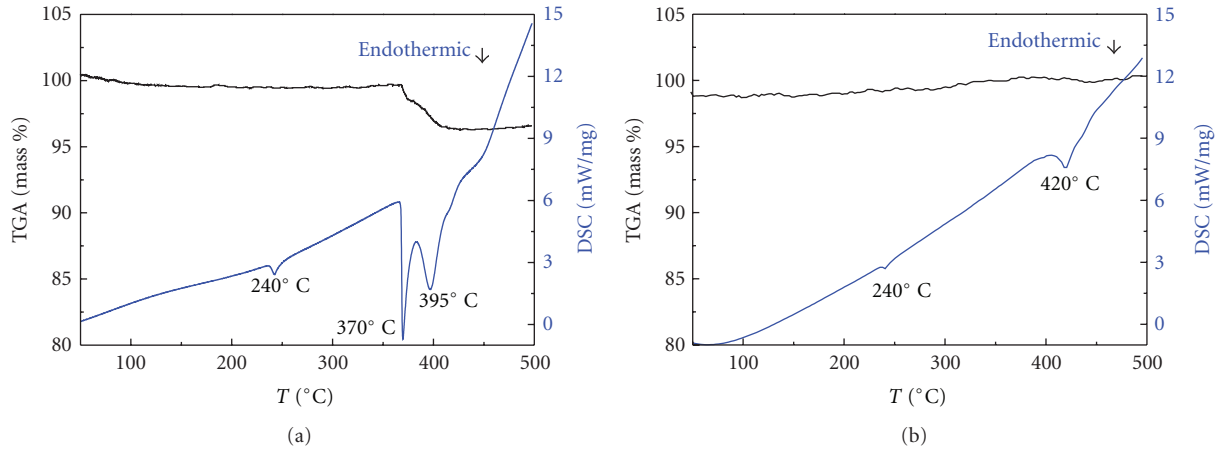

Figure 6: TG/DSC curves of the hydrogenated Mg-Ni composite samples (a) after absorbing hydrogen in 4 MPa hydrogen atmosphere at 400°C and (b) after absorbing 0.89 wt% of hydrogen at 350°C.

hydrogenated sample is MgH_2. Therefore, the hydrogenation enthalpy calculated from the lower plateaus on the P-C-T curves actually comes from the formation of both MgH_2 (majority) and Mg_2NiH_4 (minority) phases. Figure 6(b) shows the TG/DSC curves of the partially hydrided Mg-Ni composite. In Figure 6(b), two peaks are visible. A very weak endothermic peak appeared at 240°C, which corresponds to the phase transformation of Mg_2NiH_4. The other endothermic peak, with the onset point at 390°C and the peak point located at 420°C, must come from the dehydriding of MgH_2. Therefore, the endothermic peak located at 370°C observed in Figure 6(a) is confirmed from the dehydriding reaction of $Mg_2NiH_4 \rightarrow Mg_2Ni + 2H_2$ while that of 395°C is from the dehydriding reaction of $MgH_2 \rightarrow Mg + H_2$. It is worth noting here that the dehydriding temperature of MgH_2 in the fully hydrogenated powders is slightly lower than the partially hydrogenated powders. Also, the measured dehydrogenation enthalpy for MgH_2 (83.1 kJ/mol H_2) is slightly higher than its formation enthalpy (77.4 kJ/mol H_2). XRD analysis showed that the difference between the partially hydrogenated Mg-Ni powders and fully hydrogenated powders lies in the amount of Mg_2NiH_4 phase. Therefore, the Mg_2NiH_4 phase may play a role for the dehydriding of MgH_2 in the hydrogenated Mg-Ni composite powders. During dehydriding process, Mg_2NiH_4 decomposes prior to the MgH_2. The decomposition of Mg_2NiH_4 into nanostructured Mg_2Ni may act as "hydrogen channels" for the decomposition of MgH_2. Similar phenomena were also observed in Mg-Nb_2O_5 system for which the Nb_2O_5 act as hydrogen channels for hydrogen sorption of Mg [20, 21].

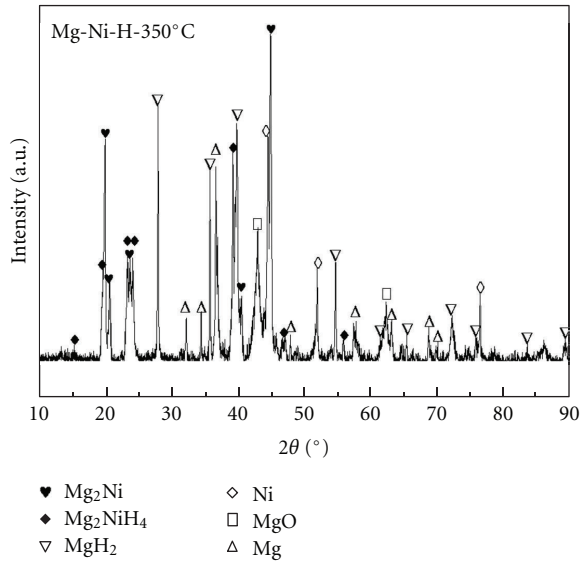

Figure 7: XRD pattern of the Mg-Ni particles after absorbing 0.89 wt% of hydrogen at 350°C.

4. Conclusions

Mg-rich Mg-Ni ultrafine powders were prepared through a DC arc plasma method. The results showed that Mg_2Ni and $MgNi_2$ phases could be obtained directly from the vapor state reactions between Mg and Ni vapors, depending on the local vapor content in the reaction chamber. After hydrogenation, a nanostructured MgH_2+Mg_2NiH_4 hydrogen storage composite could be generated from the Mg-Ni ultrafine powders. After dehydrogenation, MgH_2 and Mg_2NiH_4 decomposed into nanograined Mg and Mg_2Ni, respectively. The hydrogenation enthalpy and dehydrogenation temperature of MgH_2 in the composite are significantly reduced. TG/DSC and XRD analyses on the fully hydrogenated sample and partially hydrogenated sample showed that Mg_2NiH_4 phase may play a catalytic role in the dehydriding process of the hydrogenated Mg ultrafine particles.

Acknowledgments

Professor J. Zou would like to acknowledge the financial support from Research Funds for the Doctoral Program of Higher Education of China (no. 20100073120007) and from Shanghai Education Commission (no. 12ZZ017). This work is partly supported by projects from the Science and Technology Committee of Shanghai no. 10JC1407700, no. 11ZR1417600, and no. 10dz2211000 and "Pujiang" project no. 11PJ1406000. This work was also partially supported by the French-Chinese collaboration project "XU Guangqi" (convention no. 27847SC).

References

[1] H. Y. Shao, Y. T. Wang, H. R. Xu et al., "Preparation of Mg-based hydrogen storage materials from metal nanoparticles," *Journal of Alloys and Compounds*, vol. 465, no. 1-2, pp. 527–533, 2000.

[2] T. Z. Si, D. M. Liu, and Q. A. Zhang, "Microstructure and hydrogen storage properties of the laser sintered Mg_2Ni alloy," *International Journal of Hydrogen Energy*, vol. 32, no. 18, pp. 4912–4916, 2007.

[3] J. X. Zou, X. Q. Zeng, Y. J. Ying, P. Stephane, and W. J. Ding, "Preparation and hydrogen sorption properties of a nano-structured Mg Based Mg-La-O composite," *International Journal of Hydrogen Energy*, vol. 37, no. 17, pp. 13067–13073, 2012.

[4] N. Hanada, T. Ichikawa, and H. Fujii, "Catalytic effect of Ni nano-particle and Nb oxide on H-desorption properties in MgH_2 prepared by ball milling," *Journal of Alloys and Compounds*, vol. 404–406, pp. 716–719, 2005.

[5] T. B. Massalski, Ed., *Binary Alloy Phase Diagram*, American Society for Metals, 1986.

[6] A. A. Nayeb-Hashemi and J. B. Clark, "The Mg−Ni (Magnesium-Nickel) system," *Journal of Phase Equilibria*, vol. 6, no. 3, pp. 238–244, 1985.

[7] C. C. Koch, "Synthesis of nanostructured materials by mechanical milling: problems and opportunities," *Nanostructured Materials*, vol. 9, no. 1–8, pp. 13–22, 1997.

[8] J. Huot, H. Enoki, and E. Akiba, "Synthesis, phase transformation, and hydrogen storage properties of ball-milled $TiV_{0.9}Mn_{1.1}$," *Journal of Alloys and Compounds*, vol. 453, no. 1-2, pp. 203–209, 2008.

[9] T. Liu, H. Y. Shao, and X. G. Li, "Oxidation behaviour of Fe_3Al nanoparticles prepared by hydrogen plasma-metal reaction," *Nanotechnology*, vol. 14, no. 5, pp. 542–545, 2003.

[10] J. F. Bisson and C. Moreau, "Effect of direct-current plasma fluctuations on in-flight particle parameters: part II," *Journal of Thermal Spray Technology*, vol. 12, no. 2, pp. 258–264, 2003.

[11] S. Ohno and M. Uda, "Generation rate of ultrafine metal particles in "hydrogen plasma-metal" reaction," *Journal of the Japan Institute of Metals*, vol. 48, no. 6, pp. 640–646, 1984.

[12] H. Y. Shao, H. R. Xu, Y. T. Wang, and X. G. Li, "Preparation and hydrogen storage properties of Mg_2Ni intermetallic nanoparticles," *Nanotechnology*, vol. 15, no. 3, pp. 269–274, 2004.

[13] H. Y. Shao, T. Liu, X. G. Li, and L. F. Zhang, "Preparation of Mg_2Ni intermetallic compound from nanoparticles," *Scripta Materialia*, vol. 49, no. 6, pp. 595–599, 2003.

[14] V. Bérubé, G. Radtke, M. Dresselhaus, and G. Chen, "Size effects on the hydrogen storage properties of nanostructured metal hydrides: a review," *International Journal of Energy Research*, vol. 31, no. 6-7, pp. 637–663, 2007.

[15] G. Liang, S. Boily, J. Huot, A. V. Neste, and R. Schulz, "Hydrogen absorption properties of a mechanically milled Mg-50 wt.% $LaNi_5$ composite," *Journal of Alloys and Compounds*, vol. 268, no. 1-2, pp. 302–307, 1998.

[16] J. J. Reilly and R. H. Wiswall, "Reaction of hydrogen with alloys of magnesium and nickel and the formation of Mg_2NiH_4," *Inorganic Chemistry*, vol. 7, no. 11, pp. 2254–2256, 1968.

[17] T. R. Jensen, A. Andreasen, T. Vegge et al., "Dehydrogenation kinetics of pure and nickel-doped magnesium hydride investigated by in situ time-resolved powder X-ray diffraction," *International Journal of Hydrogen Energy*, vol. 31, no. 14, pp. 2052–2062, 2006.

[18] H. Y. Shao, Y. T. Wang, H. R. Xu, and X. G. Li, "Hydrogen storage properties of magnesium ultrafine particles prepared by hydrogen plasma-metal reaction," *Materials Science and Engineering B*, vol. 110, no. 2, pp. 221–226, 2004.

[19] L. Li, T. Akiyama, and J. I. Yagi, "Reaction mechanism of hydriding combustion synthesis of Mg_2NiH_4," *Intermetallics*, vol. 7, no. 6, pp. 671–677, 1999.

[20] K. F. Aguey-Zinsou, J. R. Ares Fernandez, T. Klassen, and R. Bormann, "Effect of Nb_2O_5 on MgH_2 properties during mechanical milling," *International Journal of Hydrogen Energy*, vol. 32, no. 13, pp. 2400–2407, 2007.

[21] G. Barkhordarian, T. Klassen, and R. Bormann, "Fast hydrogen sorption kinetics of nanocrystalline Mg using Nb_2O_5 as catalyst," *Scripta Materialia*, vol. 49, no. 3, pp. 213–217, 2003.